

Published in final edited form as:

Nat Med. 2004 December ; 10(12): 1384–1389. doi:10.1038/nm1137.

Adiponectin-mediated modulation of hypertrophic signals in the heart

Rei Shibata^{1,4}, Noriyuki Ouchi^{1,4}, Masahiro Ito², Shinji Kihara³, Ichiro Shiojima¹, David R Pimentel², Masahiro Kumada³, Kaori Sato¹, Stephan Schiekofer¹, Koji Ohashi³, Tohru Funahashi³, Wilson S Colucci², and Kenneth Walsh¹

¹Molecular Cardiology/Whitaker Cardiovascular Institute, Boston University School of Medicine, 715 Albany Street, W611, Boston, Massachusetts 02118, USA

²Cardiovascular Medicine Section, Department of Medicine, Boston University Medical Center, and Myocardial Biology Unit, Boston University School of Medicine, 715 Albany Street, X704, Boston, Massachusetts 02118, USA

³Department of Internal Medicine and Molecular Science, Graduate School of Medicine, Osaka University, 2-2, Yamada-oka, Suita, Osaka, 565-0871, Japan

Abstract

Patients with diabetes and other obesity-linked conditions have increased susceptibility to cardiovascular disorders¹. The adipocytokine adiponectin is decreased in patients with obesity-linked diseases². Here, we found that pressure overload in adiponectin-deficient mice resulted in enhanced concentric cardiac hypertrophy and increased mortality that was associated with increased extracellular signal-regulated kinase (ERK) and diminished AMP-activated protein kinase (AMPK) signaling in the myocardium. Adenovirus-mediated supplementation of adiponectin attenuated cardiac hypertrophy in response to pressure overload in adiponectin-deficient, wild-type and diabetic *db/db* mice. In cultures of cardiac myocytes, adiponectin activated AMPK and inhibited agonist-stimulated hypertrophy and ERK activation. Transduction with a dominant-negative form of AMPK reversed these effects, suggesting that adiponectin inhibits hypertrophic signaling in the myocardium through activation of AMPK signaling. Adiponectin may have utility for the treatment of hypertrophic cardiomyopathy associated with diabetes and other obesity-related diseases.

Obesity is strongly associated with the metabolic syndrome, type 2 diabetes, hypertension and heart disease¹. Pathological cardiac remodeling characterized by myocardial hypertrophy occurs with many obesity-related conditions^{3,4}, and diastolic dysfunction is one of the earliest clinical manifestations of insulin resistance⁵. But the molecular links between obesity and cardiac remodeling have not been clarified.

Adipose tissue can function as an endocrine organ by secreting adipocytokines that directly or indirectly affect obesity-linked disorders⁶. Adiponectin (also known as ACRP30) is a circulating adipose-derived cytokine that is downregulated in patients with obesity-linked diseases including type 2 diabetes, metabolic syndrome, coronary artery disease and hypertension^{2,7}. Adiponectin-knockout (APN-KO) mice show diet-induced insulin resistance,

© 2004 Nature Publishing Group

Correspondence should be addressed to K.W. (kxwalsh@bu.edu)..

⁴These authors equally contributed to this work.

Note: Supplementary information is available on the Nature Medicine website.

COMPETING INTERESTS STATEMENT The authors declare that they have no competing financial interests.

increased intimal hyperplasia after acute vascular injury, and impaired angiogenic responses to ischemia^{2,8-10}. Conversely, adiponectin overexpression reduces vascular lesions in a mouse model of atherosclerosis, and has vascular anti-inflammatory and proangiogenic effects. These data suggest that adiponectin acts as a modulator of obesity-linked vascular and metabolic disorders. But the role of adiponectin in the regulation of cardiac remodeling has not been examined previously.

To test the role of adiponectin in regulating cardiac hypertrophy, we subjected APN-KO mice to pressure overload caused by transverse aortic constriction (TAC). There were no significant differences in body weight or heart rate between APN-KO and wild-type mice after sham operation or TAC, and the increase in systolic blood pressure (sBP) after TAC was similar in wild-type and APN-KO mice (see Supplementary Table 1 online). By gross morphologic examination 7 d after TAC, APN-KO mice (as compared to wild-type mice) had increased left ventricular wall thickness typical of exaggerated concentric hypertrophy (Fig. 1a). Echocardiographic measurements 7 d after TAC showed decreased left ventricular end-diastolic dimension (LVEDD) and increased interventricular septum (IVS) and left ventricular posterior wall thickness (LVPW) in APN-KO mice, as compared to wild-type animals (Fig. 1b and Supplementary Table 1 online). The LVPW/LVEDD ratio increased markedly in APN-KO compared to wild-type mice after TAC, indicative of severe concentric hypertrophy. The calculated cardiac output was 14.1 ± 1.1 , 16.2 ± 1.0 , 14.0 ± 0.7 and 4.2 ± 0.2 ml/min in wild-type sham, wild-type TAC, APN-KO sham and APN-KO TAC, respectively. After TAC there was a small but statistically significant increase in heart weight/body weight ratio in APN-KO mice compared to wild-type animals (Fig. 1c). In addition, the increase in myocyte cross-sectional area in Masson trichrome-stained sections was greater in APN-KO than wild-type mice (Fig. 1d).

To confirm that the exaggerated hypertrophic response to pressure overload was a result of adiponectin deficiency, APN-KO and wild-type mice were treated with an adenoviral vector expressing adiponectin (Ad-APN) or with a control adenovirus (Ad- β gal), delivered through the jugular vein 3 d before TAC. At the time of surgery, adiponectin levels were 9.93 ± 1.08 μ g/ml in wild-type control, 18.80 ± 1.02 μ g/ml in wild-type Ad-APN, <0.05 μ g/ml in APN-KO control and 11.10 ± 0.78 in APN-KO Ad-APN. Adiponectin is present in serum in trimer, hexamer or high molecular weight (HMW) forms². The oligomer distribution of adenovirus-encoded adiponectin in the sera of APN-KO mice was similar to that of endogenous adiponectin in wild-type mice as determined by gel filtration analysis (Fig. 2a). Ad-APN treatment attenuated the TAC-induced changes in left ventricular morphology (increased IVS, increased LVPW) observed in APN-KO mice (Fig. 2b). Ad-APN also decreased heart weight/body weight ratio and myocyte cross-sectional area in this model (Fig. 2c). Mortality at 6, 7 and 14 d after TAC was higher in APN-KO compared to wild-type mice (Fig. 2d), presumably as a result of the notable decrease in cardiac output after TAC in APN-KO mice.

Ad-APN treatment also attenuated the increased IVS and LVPW response to TAC in *db/db* mice, which lack a functional leptin receptor, a model of obesity and diabetes (Fig. 2e). Finally, APN-KO mice subjected to angiotensin II (AngII) infusion exhibited increased IVS and LVPW compared to AngII-infused wild-type mice (Fig. 2f). The increase in sBP after AngII infusion was similar in wild-type and APN-KO mice (130.8 ± 2.4 mmHg in wild-type versus 134.4 ± 3.1 mmHg in APN-KO mice). Ad-APN treatment attenuated the AngII-induced changes in left ventricular morphology observed in both the APN-KO and wild-type mice (Fig. 2f). Thus, adiponectin supplementation was antihypertrophic in several models of pathological heart growth.

To examine the effects of adiponectin in cardiac myocytes at the cellular level, ventricular myocytes obtained from rats were subjected to α -adrenergic receptor (α AR) stimulation with

norepinephrine in the presence of propranolol (Pro)¹¹, with or without the addition of recombinant adiponectin protein. α AR stimulation for 48 h caused an increase in myocyte size and protein synthesis that was associated with reorganization of sarcomeric actin (Fig. 3a,b), and these effects were prevented by pretreatment with adiponectin. Adiponectin alone had no effect on myocyte size, protein synthesis or actin organization. Adiponectin treatment also suppressed AngII-stimulated myocyte hypertrophy (data not shown).

Gq-dependent activation of ERK is an important mediator of myocyte hypertrophy in response to pressure overload¹² and α AR stimulation¹¹. Therefore, the effect of adiponectin on ERK phosphorylation at Thr202 and Tyr204 was investigated by western blotting. *In vivo*, ERK phosphorylation was similar in myocardium from sham-operated APN-KO and wild-type mice, whereas pressure overload-induced ERK phosphorylation was enhanced in APN-KO compared to wild-type mice (Fig. 3c). In cultured cardiac myocytes, α AR stimulation induced ERK phosphorylation that was suppressed by pretreatment with adiponectin (Fig. 3d). Under the conditions of these assays, treatment with the MEK inhibitor U0126 reduced α AR-induced hypertrophy by 82% ($P < 0.01$ versus control), indicating that ERK inhibition by adiponectin contributes to the suppression of cardiac myocyte hypertrophy. Adiponectin treatment alone had no effect on ERK phosphorylation in cardiac myocytes. Adiponectin treatment also suppressed AngII-stimulated ERK phosphorylation (data not shown). The trimer form specifically suppressed α AR-stimulated ERK phosphorylation, whereas the hexamer or HMW forms of adiponectin had little effect (Fig. 3e). The trimer form of adiponectin also blocked the increase in myocyte size caused by α AR stimulation (data not shown). In contrast, the HMW form of adiponectin appears to be specific for its vascular-protective actions¹³.

Because adiponectin functions to induce AMPK signaling in many cell types including skeletal muscle, liver, adipocytes and endothelial cells^{14–17}, the phosphorylation of AMPK at Thr172 of its α subunit was assessed by western blotting. Treatment with a physiological concentration of adiponectin stimulated the phosphorylation of AMPK in cultured cardiac myocytes in a time-dependent manner (Fig. 4a). Among the three oligomeric forms of adiponectin, only the trimer stimulated AMPK phosphorylation (Fig. 4b). Conversely, AMPK phosphorylation was attenuated in APN-KO compared to wild-type hearts in both sham operation and TAC conditions (Fig. 4c). To test whether AMPK is involved in the inhibitory effects of adiponectin on myocyte hypertrophy, cultured cardiac myocytes were transduced with an adenoviral vector expressing a c-Myc-tagged dominant-negative mutant of AMPK (Ad-dnAMPK). Transduction with Ad-dnAMPK suppressed adiponectin-induced AMPK phosphorylation and acetyl-CoA carboxylase (ACC) phosphorylation (Fig. 4d). Quantitative measurements of multiple blots revealed that Ad-dnAMPK reduced AMPK and ACC phosphorylation by 97% and 90%, respectively, at the 60-min time point ($P < 0.01$ versus control). Transduction with Ad-dnAMPK also prevented the inhibitory effect of exogenous adiponectin on α AR-stimulated myocyte hypertrophy and ERK phosphorylation (Fig. 4e,f). Ad-dnAMPK alone had no effect on myocyte size, protein synthesis or ERK phosphorylation. Collectively, these data suggest that adiponectin exerts its inhibitory effect on hypertrophic signaling through activation of AMPK.

The present study shows that the fat-derived factor adiponectin can modulate cardiac remodeling. Concentric hypertrophy and diastolic dysfunction are frequently observed in diabetes and other obesity-related disorders that are associated with hypoadiponectinemia^{2–5}. The findings reported here suggest that hypoadiponectinemia may contribute to the development of pathologic cardiac hypertrophy in such patients, and that procedures to restore or increase plasma adiponectin levels could potentially be beneficial for the prevention of pathological cardiac remodeling in disorders associated with obesity.

The ability of adiponectin to attenuate cardiac hypertrophy is likely due to its ability to stimulate AMPK-dependent signaling within cardiac myocytes¹⁸. AMPK is a stress-activated protein kinase that participates in the regulation of energy and metabolic homeostasis^{19–21}. AMPK activity is increased during acute and chronic stresses such as hypoxia, ischemia and cardiac hypertrophy^{19–22}. Adiponectin can also stimulate AMPK signaling in endothelial cells^{13, 17}, but no difference in capillary density was seen between wild-type and APN-KO hearts after TAC (data not shown), suggesting that changes in myocyte signaling mediate the cardioprotective actions of adiponectin. In cardiac myocytes, adiponectin-stimulated AMPK activation suppressed ERK activation, an important prohypertrophic signaling step^{11, 12, 23}. These observations suggest that the adiponectin-AMPK signaling axis serves as a functional link between adipose tissue and the heart, and thereby influences the extent of cardiac remodeling in obesity-linked conditions.

METHODS

Materials

Phospho-AMPK (Thr172), pan- α -AMPK and phospho-p42/44 ERK (Thr202/Tyr 204) and total ERK antibodies and U0126 were purchased from Cell Signaling Technology. Tubulin antibody was from Oncogene. Phospho-ACC (Ser79), ACC and c-Myc tag antibody were purchased from Upstate Biotechnology. L-norepinephrine, DL-propranolol and AngII were purchased from Sigma. Recombinant mouse adiponectin was prepared as described previously¹⁷. Adenovirus vectors containing the gene for β -galactosidase (Ad- β gal), full-length mouse adiponectin (Ad-APN), and dominant-negative AMPK α 2 (Ad-dnAMPK) were prepared as described previously^{8, 19}. The trimer, hexamer and HMW forms of adiponectin were prepared as described previously¹³.

Transverse aortic constriction

We used adiponectin knockout (APN-KO), wild-type and *db/db* mice in a C57/BL6 background⁸. Study protocols were approved by the Institutional Animal Care and Use Committee at Boston University. Mice, at the ages of 7–11 weeks, were anesthetized with sodium pentobarbital (50 mg/kg intraperitoneally). The chest was opened, and following blunt dissection through the intercostal muscles, the thoracic aorta was identified. A 7–0 silk suture was placed around the transverse aorta and tied around a 26-gauge blunt needle, which was subsequently removed²⁴. Sham-operated mice underwent a similar surgical procedure without constriction of the aorta. After 7 d, we subjected surviving mice to transthoracic echocardiography and cardiac catheterization to determine heart rate and proximal aortic pressure. Animals were then killed and the hearts were weighed.

Adenovirus-mediated gene transfer

We injected 2×10^8 plaque-forming units (p.f.u.) of Ad-APN or Ad- β gal into the jugular vein of mice 3 d prior to TAC. We performed echocardiography 3 d after surgery. We determined mouse adiponectin levels by ELISA kit (Otsuka Pharmaceutical Co. Ltd.). The oligomeric state of adiponectin was analyzed by gel filtration chromatography as described previously¹³.

AngII infusion

We subcutaneously infused AngII (3.2mg/kg/d) into APN-KO and wild-type mice using an implanted osmotic minipump (Durect Corporation). We transduced some mice with 2×10^8 p.f.u. of Ad-APN or Ad- β gal injected into the jugular vein. After 14 d, mice were subjected to transthoracic echocardiography and cardiac catheterization to determine heart rate and blood pressure.

Echocardiography

To measure left ventricular wall thickness and chamber dimensions, we performed echocardiography with an Acuson Sequoia C-256 machine using a 15-MHz probe. After we obtained a two-dimensional image, we measured M-mode images of the left ventricular posterior wall thickness. We calculated cardiac output by the cubed method ($1.047 \times (LVEDD^3 - LVESD^3) \times \text{heart rate}$).

Cell culture and adenoviral infection

Primary cultures of the neonatal rat ventricular myocytes were prepared as described previously²³. The isolated myocytes were cultured in Dulbecco Modified Eagle medium containing 7% fetal calf serum. Before each experiment, we placed cells in serum-free Dulbecco Modified Eagle medium for 24 h. For the adiponectin stimulation studies, we treated with 30 $\mu\text{g/ml}$ of mouse recombinant adiponectin for the indicated lengths of time. Experiments for norepinephrine stimulation were performed by treating cells with 30 $\mu\text{g/ml}$ of mouse recombinant adiponectin or vehicle for 30 min. We then treated cells with 2 μM of propranolol for 30 min and stimulated with 1 μM norepinephrine for the indicated lengths of time. In some experiments, we infected the cells with Ad- βgal and Ad-dnAMPK at a multiplicity of infection of 50 for 24 h before treatments. Myocyte surface area was assessed using semi-automatic computer-assisted planimetry (Bioquant) from two-dimensional images of unstained cells. [³H]-leucine incorporation was determined as previously described²⁴.

Immunohistochemical analysis

Mice were killed and left ventricular tissue was obtained 7 d after TAC. We embedded tissue in OCT compound (Miles) and snap-froze it in liquid nitrogen. We then prepared tissue slices (5 μm). Tissue sections were stained with hematoxylin and eosin or with Masson trichrome. We calculated the myocyte cross-sectional area by measuring 200 cells per section. To determine sarcomeric F-actin organization, we stained cultured myocytes with FITC-conjugated phalloidin (Sigma).

Western blot analysis

Heart tissue samples obtained on day 7 after surgery were homogenized in lysis buffer containing 20 mM Tris-HCl (pH 8.0), 1% NP-40, 150 mM NaCl, 0.5% deoxycholic acid, 1 mM sodium orthovanadate, and protease inhibitor cocktail (Sigma). We homogenized rat myocytes in the same lysis buffer. Protein (50 μg) was separated with denaturing SDS 10% polyacrylamide gels. After transfer of protein to membranes, we performed immunoblot analysis with the indicated antibodies at a 1:1,000 dilution. This was followed by incubation with secondary antibody conjugated with horseradish peroxidase at a 1:5,000 dilution. We used the ECL Western Blotting Detection kit (Amersham Pharmacia Biotech) for detection.

Statistical analysis

Data are presented as mean \pm s.e.m. or s.d. as indicated in the figure legends. Statistical analysis was performed by student's *t*-test, Scheffe's F test and χ^2 analysis. A value of $P < 0.05$ was accepted as statistically significant.

Supplementary Material

Refer to Web version on PubMed Central for supplementary material.

Acknowledgments

We acknowledge the technical assistance of S. Tanaka and A. Bialik. This work was supported by US National Institutes of Health (NIH) grants HL66957, AR40197, AG15052 and AG17241 to K. Walsh, HL61639 and HL20612 to W.S. Colucci, NIH Cardiovascular Scientist Training Grant HL07224 to D.R. Pimentel; and grants from the Japanese Ministry of Education and the Japan Society for Promotion of Science-Research for the Future Program. R. Shibata, N. Ouchi and M. Ito were supported by grants from the Uehara Memorial Foundation.

References

1. Reilly MP, Rader DJ. The metabolic syndrome: more than the sum of its parts? *Circulation* 2003;108:1546–1551. [PubMed: 14517150]
2. Ouchi N, Kihara S, Funahashi T, Matsuzawa Y, Walsh K. Obesity, adiponectin and vascular inflammatory disease. *Curr. Opin. Lipidol* 2003;14:561–566. [PubMed: 14624132]
3. Iltercil A, et al. Relationship of impaired glucose tolerance to left ventricular structure and function: The Strong Heart Study. *Am. Heart J* 2001;141:992–998. [PubMed: 11376315]
4. Rutter MK, et al. Impact of glucose intolerance and insulin resistance on cardiac structure and function: sex-related differences in the Framingham Heart Study. *Circulation* 2003;107:448–454. [PubMed: 12551870]
5. Schannwell CM, Schneppenheim M, Perings S, Plehn G, Strauer BE. Left ventricular diastolic dysfunction as an early manifestation of diabetic cardiomyopathy. *Cardiology* 2002;98:33–39. [PubMed: 12373045]
6. Kahn BB, Flier JS. Obesity and insulin resistance. *J. Clin. Invest* 2000;106:473–481. [PubMed: 10953022]
7. Scherer PE, Williams S, Fogliano M, Baldini G, Lodish HF. A novel serum protein similar to C1q, produced exclusively in adipocytes. *J. Biol. Chem* 1995;270:26746–26749. [PubMed: 7592907]
8. Maeda N, et al. Diet-induced insulin resistance in mice lacking adiponectin/ACRP30. *Nat. Med* 2002;8:731–737. [PubMed: 12068289]
9. Kubota N, et al. Disruption of adiponectin causes insulin resistance and neointimal formation. *J. Biol. Chem* 2002;277:25863–25866. [PubMed: 12032136]
10. Shibata R, et al. Adiponectin stimulates angiogenesis in response to tissue ischemia through stimulation of amp-activated protein kinase signaling. *J. Biol. Chem* 2004;279:28670–28674. [PubMed: 15123726]
11. Xiao L, et al. MEK1/2-ERK1/2 mediates alpha1-adrenergic receptor-stimulated hypertrophy in adult rat ventricular myocytes. *J. Mol. Cell. Cardiol* 2001;33:779–787. [PubMed: 11273730]
12. Esposito G, et al. Cardiac overexpression of a G(q) inhibitor blocks induction of extracellular signal-regulated kinase and c-Jun NH(2)-terminal kinase activity in *in vivo* pressure overload. *Circulation* 2001;103:1453–1458. [PubMed: 11245652]
13. Kobayashi H, et al. Selective suppression of endothelial cell apoptosis by the high molecular weight form of adiponectin. *Circ. Res* 2004;94:e27–e31. [PubMed: 14752031]
14. Tomas E, et al. Enhanced muscle fat oxidation and glucose transport by ACRP30 globular domain: acetyl-CoA carboxylase inhibition and AMP-activated protein kinase activation. *Proc. Natl. Acad. Sci. USA* 2002;99:16309–16313. [PubMed: 12456889]
15. Yamauchi T, et al. Adiponectin stimulates glucose utilization and fatty-acid oxidation by activating AMP-activated protein kinase. *Nat. Med* 2002;8:1288–1295. [PubMed: 12368907]
16. Wu X, et al. Involvement of AMP-activated protein kinase in glucose uptake stimulated by the globular domain of adiponectin in primary rat adipocytes. *Diabetes* 2003;52:1355–1363. [PubMed: 12765944]
17. Ouchi N, et al. Adiponectin stimulates angiogenesis by promoting cross-talk between AMP-activated protein kinase and Akt signaling in endothelial cells. *J. Biol. Chem* 2004;279:1304–1309. [PubMed: 14557259]
18. Chan AY, Soltys CL, Young ME, Proud CG, Dyck JR. Activation of AMP-activated protein kinase inhibits protein synthesis associated with hypertrophy in the cardiac myocyte. *J. Biol. Chem* 2004;279:32771–32779. [PubMed: 15159410]

19. Nagata D, Mogi M, Walsh K. AMP-activated protein kinase (AMPK) signaling in endothelial cells is essential for angiogenesis in response to hypoxic stress. *J. Biol. Chem* 2003;278:31000–31006. [PubMed: 12788940]
20. Mu J, Brozinick JT Jr, Valladares O, Bucan M, Birnbaum MJ. A role for AMP-activated protein kinase in contraction- and hypoxia-regulated glucose transport in skeletal muscle. *Mol. Cell* 2001;7:1085–1094. [PubMed: 11389854]
21. Kudo N, Barr AJ, Barr RL, Desai S, Lopaschuk GD. High rates of fatty acid oxidation during reperfusion of ischemic hearts are associated with a decrease in malonyl-CoA levels due to an increase in 5'-AMP-activated protein kinase inhibition of acetyl-CoA carboxylase. *J. Biol. Chem* 1995;270:17513–17520. [PubMed: 7615556]
22. Tian R, Musi N, D'Agostino J, Hirshman MF, Goodyear LJ. Increased adenosine monophosphate-activated protein kinase activity in rat hearts with pressure-overload hypertrophy. *Circulation* 2001;104:1664–1669. [PubMed: 11581146]
23. Pimentel DR, et al. Reactive oxygen species mediate amplitude-dependent hypertrophic and apoptotic responses to mechanical stretch in cardiac myocytes. *Circ. Res* 2001;89:453–460. [PubMed: 11532907]
24. Rogers JH, et al. RGS4 causes increased mortality and reduced cardiac hypertrophy in response to pressure overload. *J. Clin. Invest* 1999;104:567–576. [PubMed: 10487771]

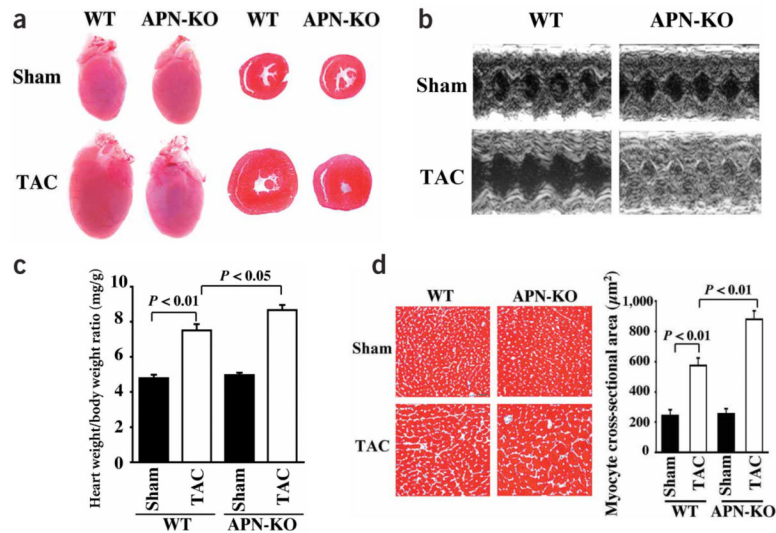
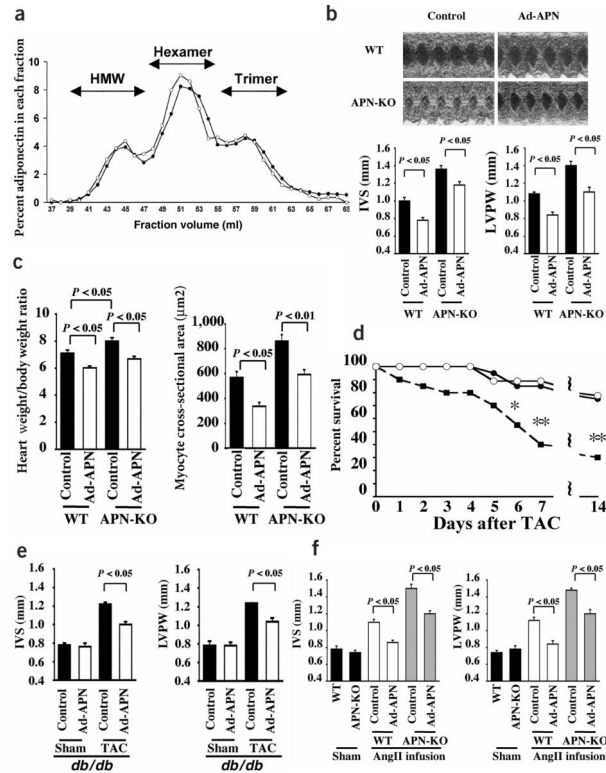


Figure 1.

Enhanced pressure overload-induced cardiac hypertrophy in APN-KO mice subjected to TAC. **(a)** Representative pictures of hearts from wild-type (WT) and APN-KO mice at 7 d after sham operation or TAC (left). Representative hematoxylin and eosin-stained cross-sections of left ventricular myocardium from wild-type and APN-KO mice 7 d after sham operation or TAC (right). **(b)** Representative M-mode echocardiogram for APN-KO and wild-type (WT) mice 7 d after sham operation or TAC. **(c)** Heart weight/body weight ratio in wild-type ($n = 6$) and knockout mice ($n = 5$) 7 d after sham operation or TAC. **(d)** Histological analysis of heart sections from wild-type and APN-KO mice stained with Masson trichrome (magnification, $\times 400$; bar indicates $50 \mu\text{m}$). Quantitative analysis of cardiac myocyte cross-sectional area ($n = 200$ per section) in wild-type ($n = 6$) and APN-KO mice ($n = 5$). Results are presented as mean \pm s.e.m.

**Figure 2.**

Adenovirus-mediated supplementation of adiponectin protects against the development of cardiac hypertrophy. **(a)** Oligomeric state of adenovirus-delivered adiponectin in APN-KO mouse (open circle) and endogenous adiponectin in wild-type mouse (closed circles) assessed by gel filtration analysis. The adenoviral vector expressing adiponectin (Ad-APN, 2×10^8 p.f.u. total) was delivered through the jugular vein, and the oligomeric state of adiponectin was analyzed 3 d after Ad-APN injection. **(b)** Adenovirus-mediated supplementation of adiponectin in APN-KO and wild-type (WT) mice attenuated cardiac hypertrophy in response to TAC as shown by echocardiography. Adenoviral vectors expressing adiponectin (Ad-APN, 2×10^8 p.f.u. total, $n = 3$) or β -galactosidase (control, $n = 3$) were delivered intravenously through the jugular vein 3 d before TAC surgery. Left ventricular wall thickness (IVS and LVPW) was determined at 3 d after TAC. **(c)** Heart weight/body weight ratio and cardiac myocyte cross-sectional area in wild-type ($n = 5$) and knockout mice ($n = 3$) treated with Ad-APN or Ad- β gal (control) were determined at 7 d after sham operation or TAC. **(d)** Decreased survival of APN-KO mice (closed squares) after TAC ($n = 20$; $*P < 0.05$, $**P < 0.01$) in comparison with wild-type mice (closed circles) after TAC ($n = 20$). Adenovirus-mediated supplementation of adiponectin in APN-KO ($n = 9$) (open circles) improved survival to a level that is comparable to that of wild-type mice. **(e)** Adenovirus-mediated supplementation of adiponectin in diabetic *db/db* mice attenuated cardiac hypertrophy in response to TAC as shown by echocardiography. Ad-APN (2×10^8 p.f.u. total, $n = 4$) or β -galactosidase (control, $n = 4$) were delivered intravenously through the jugular vein 3 d before TAC surgery. Wall thickness (IVS and LVPW) was determined at 3 d after TAC surgery or sham operation. **(f)** APN-KO mice showed an increased cardiac hypertrophy following AngII infusion relative to wild-type mice ($n = 4$). Adenovirus-mediated supplementation of adiponectin (2×10^8 p.f.u.) in APN-KO ($n = 4$) and wild-type ($n = 4$) mice attenuated AngII-induced cardiac hypertrophy. Wall thickness (IVS and LVPW) was determined after 14 d of AngII infusion. Results are presented as mean \pm s.e.m.

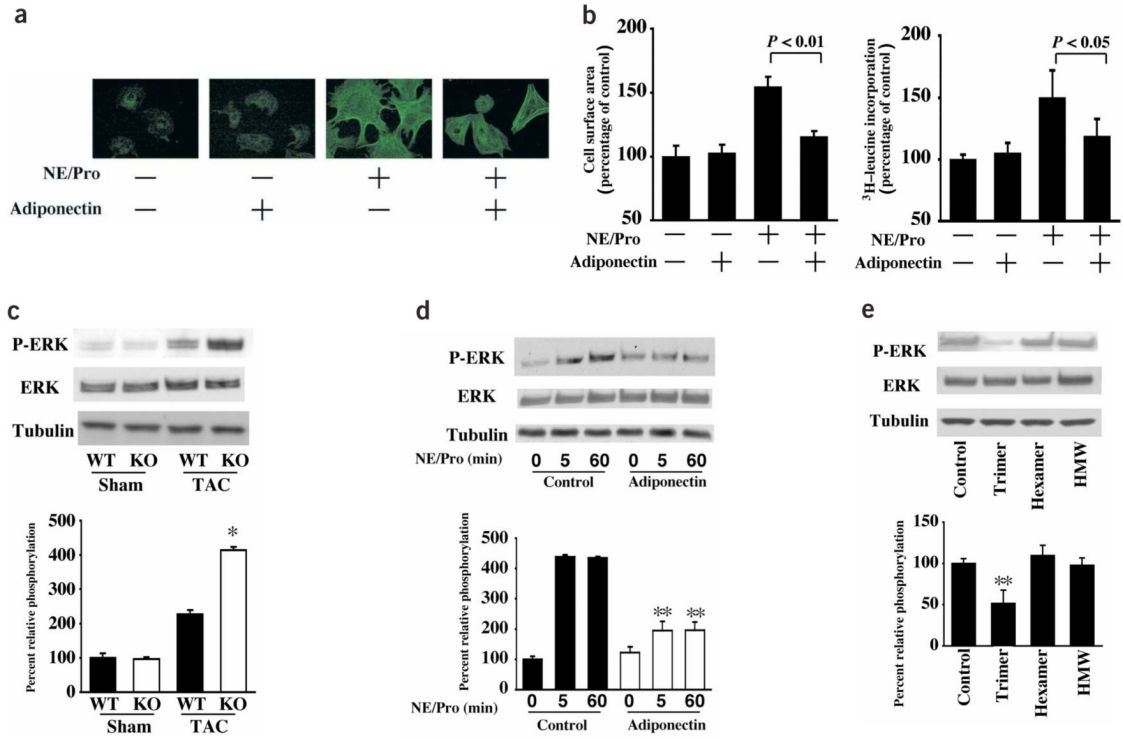


Figure 3. Adiponectin inhibits the hypertrophic response to α AR stimulation or pressure overload. **(a)** Representative example of immunostaining of sarcomeric F-actin with rhodamine phalloidin in rat cardiac myocytes. Cells were pretreated with adiponectin (30 μ g/ml) or vehicle for 30 min, Pro (2 μ M) for an additional 30 min, followed by the addition of norepinephrine (NE) for 48 h. **(b)** Quantitative analysis of cell surface area measured by semi-automatic computer-assisted planimetry (Bioquant) from two-dimensional images of 100 cells selected at random (left) and protein synthesis measured by [³H]-leucine incorporation (right). **(c)** The phosphorylation (P-) of ERK in heart tissues from wild-type and APN-KO mice at 7 d after sham operation or TAC. **(d)** Effect of adiponectin on the phosphorylation of ERK in response to α AR-stimulation in cultured rat cardiac myocytes. Cells were pretreated with adiponectin (30 μ g/ml) or vehicle for 30 min, 2 μ M Pro for an additional 30 min and then stimulated with or without 1 μ M norepinephrine (NE) for the indicated length of time. **(e)** Effects of three different oligomeric forms of adiponectin on the phosphorylation of ERK in response to α AR-stimulation in cultured rat cardiac myocytes. Cells were pretreated with each form of adiponectin (5 μ g/ml) or vehicle for 30 min, 2 μ M Pro for an additional 30 min and then stimulated with 1 μ M NE for 5 min. Relative phosphorylation levels of ERK were quantified using the US National Institutes of Health image program. Immunoblots were normalized to total loaded protein. Results are presented as mean \pm s.d. ($n = 3-6$). * $P < 0.05$ versus wild-type. ** $P < 0.05$ versus control.

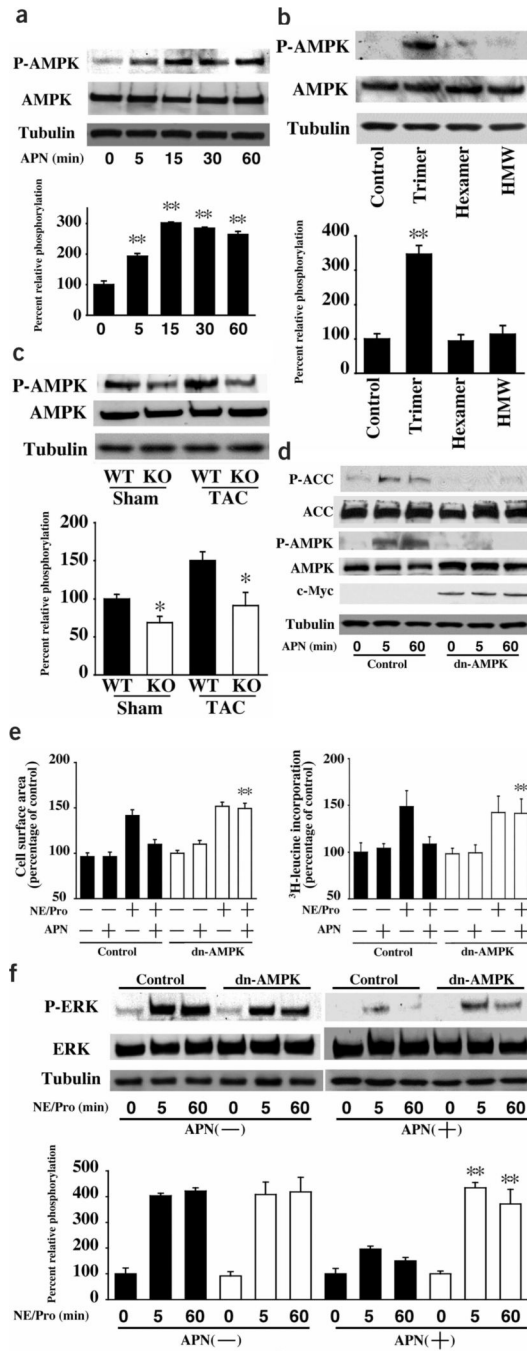


Figure 4. Adiponectin inhibition α AR-stimulated myocyte hypertrophy is mediated through AMPK signaling. (a) Time-dependent changes in the phosphorylation of AMPK in rat cultured cardiac myocytes after adiponectin treatment (30 μ g/ml). (b) Effects of three different oligomeric forms of adiponectin (5 μ g/ml) on the phosphorylation of AMPK. (c) The phosphorylation of AMPK in myocardium from wild-type (WT) and APN-KO mice at 7 d after sham operation or TAC. (d) Ad-dnAMPK reversed adiponectin stimulation of AMPK and ACC phosphorylation. Rat cardiac myocytes were transduced with c-Myc-tagged Ad-dnAMPK or Ad- β gal (control) at a multiplicity of infection of 50 for 24 h in serum-starved media. Cells were treated with adiponectin (30 μ g/ml) for the indicated lengths of time. (e) Contribution of AMPK signaling

to the inhibitory effect of adiponectin on α AR-stimulated myocyte hypertrophy. After 24-h transduction of rat cardiac myocytes with Ad-dnAMPK or Ad- β gal (control), cells were pretreated with adiponectin (30 μ g/ml) or vehicle for 30 min and then treated with 2 μ M Pro for 30 min and stimulated with or without 1 μ M norepinephrine (NE) for 48 h. Quantitative analysis of cell surface area was performed in 100 randomly selected cells (left) or 3 H-leucine incorporation into protein (right). **(f)** Effect of Ad-dnAMPK on adiponectin inhibition of NE/Pro-induced ERK phosphorylation. Cells were treated as in **e** and then stimulated with or without 1 μ M norepinephrine (NE) for the indicated lengths of time. Relative phosphorylation levels of AMPK and ERK were quantified using the US National Institutes of Health image program. Immunoblots were normalized to total loaded protein. Results are presented as mean \pm s.d. ($n = 3-5$). * $P < 0.05$ versus wild-type. ** $P < 0.05$ versus control.